NASA/TM—2012–217462

Systematic Destruction of Electronic Parts for Aid in Electronic Failure Analysis

S.E. Decker, T.D. Rolin, and P.D. McManus
NASA Marshall Space Flight Center, Huntsville, Alabama

June 2012

The NASA STI Program…in Profile

Since its founding, NASA has been dedicated to the advancement of aeronautics and space science. The NASA Scientific and Technical Information (STI) Program Office plays a key part in helping NASA maintain this important role.

The NASA STI Program Office is operated by Langley Research Center, the lead center for NASA's scientific and technical information. The NASA STI Program Office provides access to the NASA STI Database, the largest collection of aeronautical and space science STI in the world. The Program Office is also NASA's institutional mechanism for disseminating the results of its research and development activities. These results are published by NASA in the NASA STI Report Series, which includes the following report types:

- TECHNICAL PUBLICATION. Reports of completed research or a major significant phase of research that present the results of NASA programs and include extensive data or theoretical analysis. Includes compilations of significant scientific and technical data and information deemed to be of continuing reference value. NASA's counterpart of peer-reviewed formal professional papers but has less stringent limitations on manuscript length and extent of graphic presentations.

- TECHNICAL MEMORANDUM. Scientific and technical findings that are preliminary or of specialized interest, e.g., quick release reports, working papers, and bibliographies that contain minimal annotation. Does not contain extensive analysis.

- CONTRACTOR REPORT. Scientific and technical findings by NASA-sponsored contractors and grantees.

- CONFERENCE PUBLICATION. Collected papers from scientific and technical conferences, symposia, seminars, or other meetings sponsored or cosponsored by NASA.

- SPECIAL PUBLICATION. Scientific, technical, or historical information from NASA programs, projects, and mission, often concerned with subjects having substantial public interest.

- TECHNICAL TRANSLATION. English-language translations of foreign scientific and technical material pertinent to NASA's mission.

Specialized services that complement the STI Program Office's diverse offerings include creating custom thesauri, building customized databases, organizing and publishing research results…even providing videos.

For more information about the NASA STI Program Office, see the following:

- Access the NASA STI program home page at <http://www.sti.nasa.gov>

- E-mail your question via the Internet to <help@sti.nasa.gov>

- Fax your question to the NASA STI Help Desk at 443–757–5803

- Phone the NASA STI Help Desk at 443–757–5802

- Write to:
  NASA STI Help Desk
  NASA Center for AeroSpace Information
  7115 Standard Drive
  Hanover, MD 21076–1320

NASA/TM—2012–217462

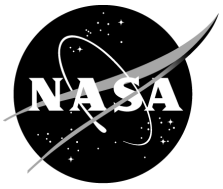

Systematic Destruction of Electronic Parts for Aid in Electronic Failure Analysis

S.E. Decker, T.D. Rolin, and P.D. McManus
NASA Marshall Space Flight Center, Huntsville, Alabama

National Aeronautics and
Space Administration

Marshall Space Flight Center • Huntsville, Alabama 35812

June 2012

Available from:

NASA Center for AeroSpace Information
7115 Standard Drive
Hanover, MD 21076–1320
443–757–5802

This report is also available in electronic form at
<https://www2.sti.nasa.gov/login/wt/>

TABLE OF CONTENTS

LIST OF FIGURES

LIST OF FIGURES (Continued)

LIST OF FIGURES (Continued)

LIST OF TABLES

ACRONYMS AND ABBREVIATIONS

AUX	auxiliary
DIV	division
DPA	destructive physical analysis
EEE	electrical, electronic, and electromechanical
EOS	electrical overstress
HORIZ	horizontal
LDC	lot date code
NPN	Negative-Positive-Negative
op amp	operational amplifier
PNP	Positive-Negative-Positive
VERT	vertical

TECHNICAL MEMORANDUM

SYSTEMATIC DESTRUCTION OF ELECTRONIC PARTS FOR AID IN ELECTRONIC FAILURE ANALYSIS

1. INTRODUCTION

Electrical, electronic, and electromechanical (EEE) parts are critical to virtually all of NASA's missions. When a critical part fails, it costs time and money, jeopardizes safety, and can even compromise the success of a mission. It is important to know why a certain part failed so the problem can be corrected and avoided in the future. Because there are numerous reasons that parts fail, failure analysts have to employ a variety of techniques to investigate the failures. A simple, cost effective method of performing failure analysis requires removing the lid of a part and examining it under a microscope to look for visible signs of damage;[1] this technique is known as destructive physical analysis (DPA). To aid in this type of failure analysis, it is advantageous to become familiar with and to catalog the damage caused by a defined electrical pulse.

Research has shown that very few databases of this nature have been produced. In most cases, the effects of electrical overstresses are observed and noted as junction burnout, dielectric or oxide punch through, and metallization burnout but do not compile illustrations of the damage. For example, one report gives examples of curve trace data for failed parts but no conclusions were drawn concerning the cause of the damage.[2] Given the limited amount of data available, the analyst has to estimate voltage and time intervals based on aluminum trace condition (melted versus splattered) and glassivation condition (discolored versus cracked). In many cases, the component design can vary from part to part causing these estimates to be errant.

This study is designed to provide a technique that will aid the analyst in avoiding the inherent error in estimating electrical overstress (EOS) conditions. This objective is accomplished by providing the analyst with a simple pictorial for comparison to field failures. Not all the available components in the industry can be part of this database; however, when looking at certain parts that have common design features, a good basic understanding of the EOS failure can be developed. As a preliminary area of investigation, two different types of bipolar devices were chosen.

Figure 1 depicts images of the devices as obtained by a Keyence VHX-600 3D optical microscope. One was an operational amplifier (op amp) with part number JM38510/13501BPA and lot date code (LDC) OD9104 (see fig. 1(a)). Op amps are used in an extremely broad range of applications including amplification, filtering, nonlinear wave shaping, wave generation, and switching.[3] The other component chosen was a positive-negative-positive (PNP) transistor with part number JANTXV2N2907A and LDC 8710B (see fig. 1(b)). Transistors are commonly used to amplify signals in linear circuits, to amplify current in logic circuits, and to operate as switches.

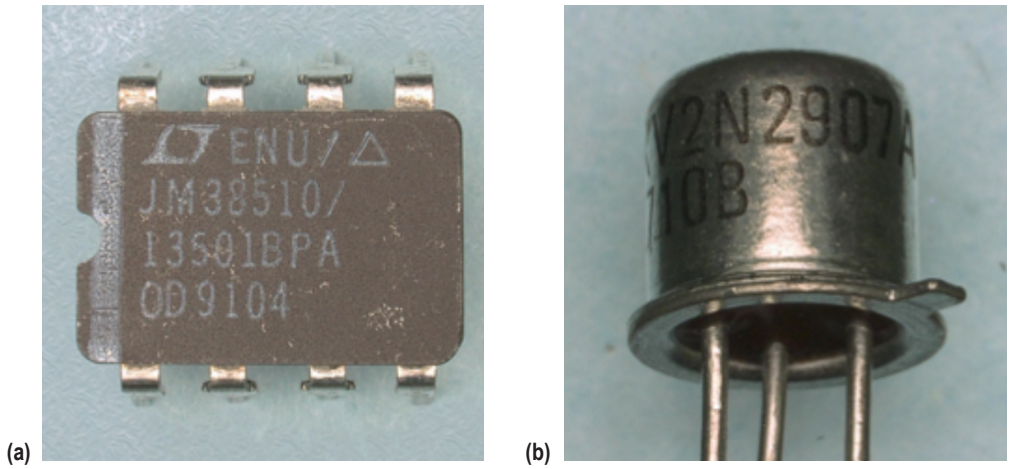

Figure 1. Keyence VHX-600 3D optical microscope images: (a) A typical JM38510/13501BPA op amp and (b) a typical JANTXV2N2907A PNP transistor.

2. BACKGROUND ON EQUIPMENT

To limit the number of variables, op amps and transistors were systematically pulsed using a known voltage over a known period of time. The pulses were generated using an AVTECH Model AVR-5B-B-RN-PN pulse generator and recorded using a Tektronix TDS 5054 Digital Phosphor Oscilloscope (see fig. 2(a)). The pulse generator is capable of generating 0–500 V into loads of 50 Ω or higher and a variable pulse width from 100 ns to 100 μs. The maximum power output of this instrument is 50 W, which limits the voltage that can be applied to the samples when high currents (shorts) are involved. The damage was assessed using a Tektronix 370B Programmable Curve Tracer (see fig. 2(b)) that measures and displays the semiconductor characteristics of the damaged parts. The samples were then opened and the damage site was photographed using a metallograph. The metallograph produces high-resolution/high-magnification photographs that make it possible to view very small damage sites on the op amps and transistors. The damage was examined using bright field, dark field, and differential interference contrast techniques. Only the bright field images were used for this paper and for the op amp and transistor catalogs because it provided the most detailed and easily interpreted view of the damage sites.

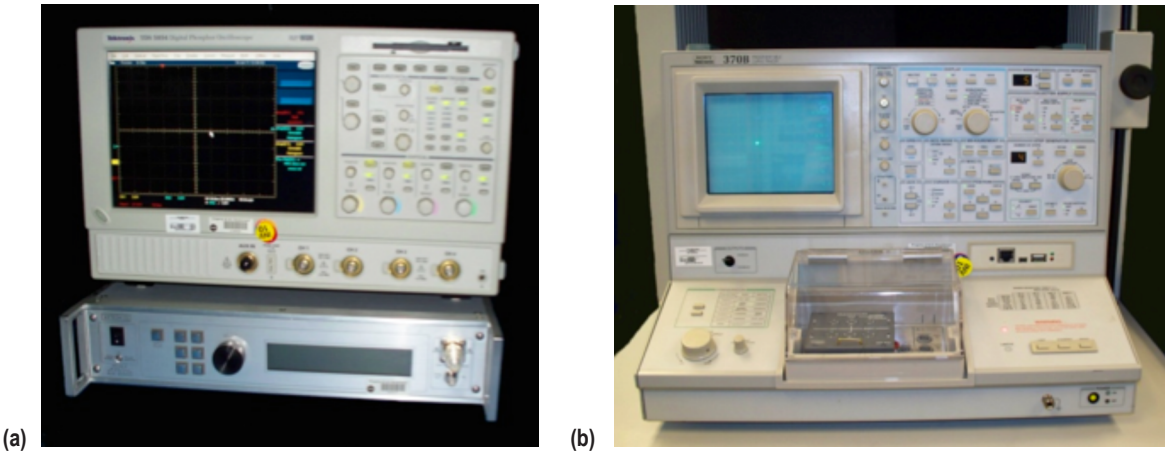

Figure 2. Pulses were generated and recorded by (a) the Tektronix TDS 5054 Digital Phosphor Oscilloscope (top) and the AVTECH Model AVR-5B-B-RN-PN Pulse Generator (bottom), and they were assessed by (b) the Tektronix 370B Programmable Curve Tracer.

3. PROCEDURE

The first step in this analysis was to find op amps with acceptable breakdown voltages and transistors with comparable high-current and low-current gains (β). The minimum breakdown voltages for these parts were obtained from the military standard data sheets and were used to set the guidelines for what was considered a 'good' part. To obtain a set of testable op amps and transistors, many parts with the same part number and LDC were evaluated on the curve tracer. The op amps and transistors that met the required breakdown voltage or current gain were assigned a sample number and their initial curve traces were recorded. Additionally, a known good transistor (see fig. 3(a)) and a known good op amp (see fig. 3(b)) were opened and photographed for comparison to damaged samples.

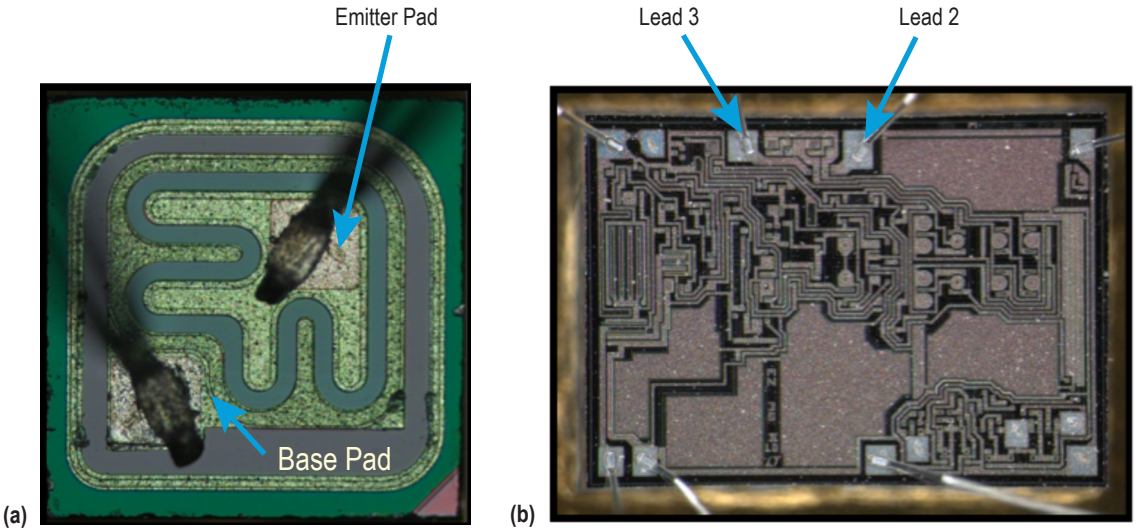

Figure 3. Depiction of (a) a known good transistor at × 20 bright field objective magnification and (b) a known good op amp at × 10 dark field objective magnification.

3.1 Operational Amplifiers

The pin diagram, also known as the pin out, of an op amp is given in figure 4(a). The op amps were all pulsed with the positive lead on pin 3 and the negative lead on pin 2, and the polarity of the pulse was programmed into the pulse generator. The other leads were not connected to confine the damage location on the internal silicon die to the area shown in figure 4(b). The pulse width, voltage, and current supplied to the op amps were recorded using an oscilloscope. The oscilloscope software was used to generate a power trace and to calculate the pulse energy applied to each sample.

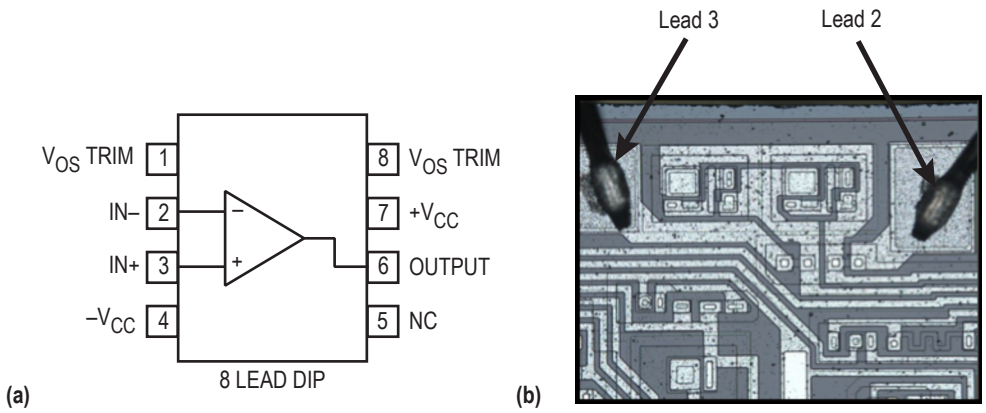

Figure 4. Pin out drawing of (a) the op amp, and pulses were applied between (b) leads 3 and 2. All damage observed was in this general location.

The op amp procedure consisted of first performing a curve trace to confirm that each sample met specifications. For these op amps, the breakdown voltage required for further testing was 750 mV (see fig. 5). The destruction of the op amps consisted of pulsing a device at a voltage and time interval that would not completely open the circuit and then adding 1 µs to the time interval for the next pulse on the next device. The time was reduced by 0.5 µs if the circuit opened on the second op amp and a third op amp was pulsed at the same voltage level. This was done for voltages between 60–100 V at 10-V intervals. A 'test' op amp was used to find a reasonable starting pulse width for each voltage change to conserve the in-family samples. Damage was initially indicated if an abrupt drop in the voltage waveform was observed on an oscilloscope. Damage was verified by evaluating the circuit using the curve tracer. The device lid was then removed and the silicon die was inspected using an optical microscope. The resulting damage was examined and photographed using a metallograph at × 20 and × 50 objective magnification.

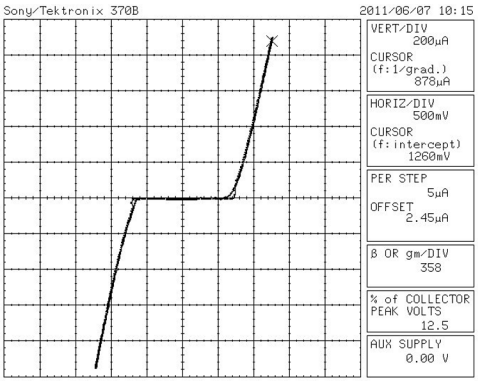

Figure 5. The curve trace between input pins 3 (+) and 2 (–) is shown for a good device. The forward and reverse breakdown voltages for the input pins are equivalent and are approximately 750 mV.

3.2 Transistors

Six sets of transistors were tested to achieve a complete range of damage on the transistors. Three of the sets were pulsed in one of the forward bias conditions (emitter to base with positive on the emitter and negative on the base, collector to base with positive on the collector and negative on the base, or collector to emitter with positive on the collector and negative on the emitter). The remaining three sets were pulsed in one of the reverse bias conditions (emitter to base with negative on the emitter and positive on the base, collector to base with negative on the collector and positive on the base, or collector to emitter with negative on the collector and positive on the emitter). The PNP transistors to be tested were chosen based on their high-current and low-current β. To be considered testable samples, the transistors had to have a high-current β between 180 and 186 (see fig. 6(a)) and a low-current β between 116 and 124 (see fig. 6(b)). The curve traces of each transistor's high-current and low-current β characteristic set of curves, along with the emitter to base and collector to base reverse breakdown voltages were recorded prior to damage.

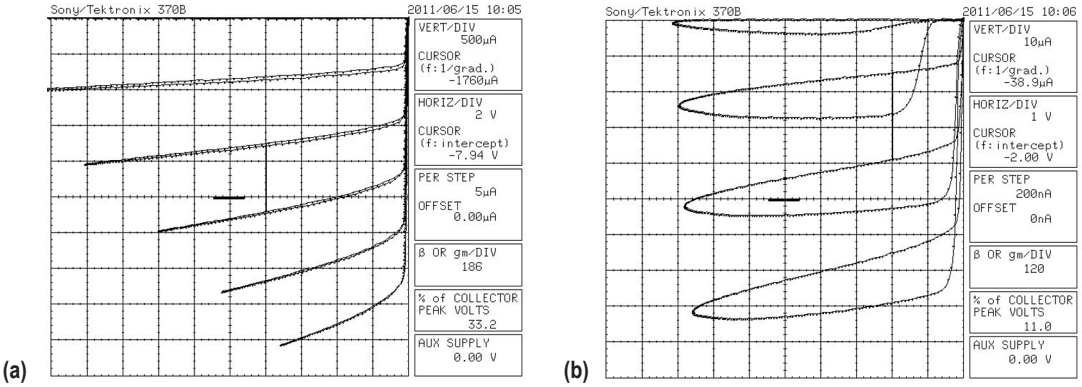

Figure 6. Examples of typical sets of (a) high-current and (b) low-current β characteristic curves for the transistors.

In figure 6, the high-current curves show a current β of 186 and the low-current curves show a current β of 120.The collector to emitter reverse breakdown voltage for each transistor sample was not recorded because the high current and high voltage required for the measurement could damage the sample. In addition, the length of time required for the curve tracer to save this data would only intensify the problem. Damage by the curve tracer is not desirable because it could compromise the pulse generator results. The military standard data sheet specification for each of the three reverse breakdown voltages and the averages of the measured values for the reverse emitter to base voltage and reverse collector to base voltage are given in table 1.

Table 1. Reverse breakdown voltages of transistor samples.

Parameter	Military Standard (V)	Measured Average (V)
Collector to emitter (VCEO)	>60	Not measured
Emitter to base (VEBO)	>5	6.5
Collector to base (VCBO)	>60	105

Transistors that did not meet the required high-current and low-current β were used to find the optimal starting voltage and pulse width for each junction tested and then removed from the test lot. The pulse width, voltage, and current supplied to the transistors were recorded using an oscilloscope. Oscilloscope software was used to generate a power trace and to calculate the pulse energy applied to each sample. The intention was for each junction to be pulsed from a point where there was still a characteristic set of curves with readable β to a point where most of the junctions were either shorted or open. After being pulsed, the transistor sample was curve traced to evaluate each junction (reverse and forward bias emitter to base, reverse and forward bias collector to base, reverse and forward bias collector to emitter, and the high-current family set of curves). The high-current family set of curves was recorded for each transistor along with either the breakdown voltage or resistance of each junction. Finally, the transistors were opened and the damage was observed using a metallograph at $\times 20$ and $\times 50$ objective magnification.

4. DATA

4.1 Operational Amplifiers

Figure 7 depicts circuit schematics and the internal die area of the op amp where the pulses were applied. A schematic drawing of the op amp is shown in figure 7(a) and a normal curve trace is shown in figure 5. The slopes of the lines in figure 5 indicate a resistance of approximately 1,000 Ω, confirming the value of 500 Ω for the series resistors shown in the circled area of figure 7(a). The pulses were applied between leads 3 and 2 (circled in blue). The protective diodes shown in the circled area of figure 7(a) are actually the base-emitter junctions of negative-positive-negative (NPN) lateral processed transistors as shown in figure 7(b). The resulting damage was optically confirmed to be confined to the two 500-Ω resistors and the four NPN transistors that are located between the second and third leads (figure 7(c)). The relevant data, including the voltage, voltage polarity, pulse width, energy, and current applied to each sample, are given in table 2.

Three typical device failure characteristics were noted (see table 2). Two of these characteristics occur when the applied pulses have energies of approximately 400 μJ or less. The first characteristic was mostly minimal damage to the op amp. Slight charring is noted in the diffused resistors in which a small amount of metal flow is observed. Curve traces show no change in the forward or reverse breakdown voltages; however, the resistances of the diffused resistors were slightly reduced from the typical value of 500 Ω.

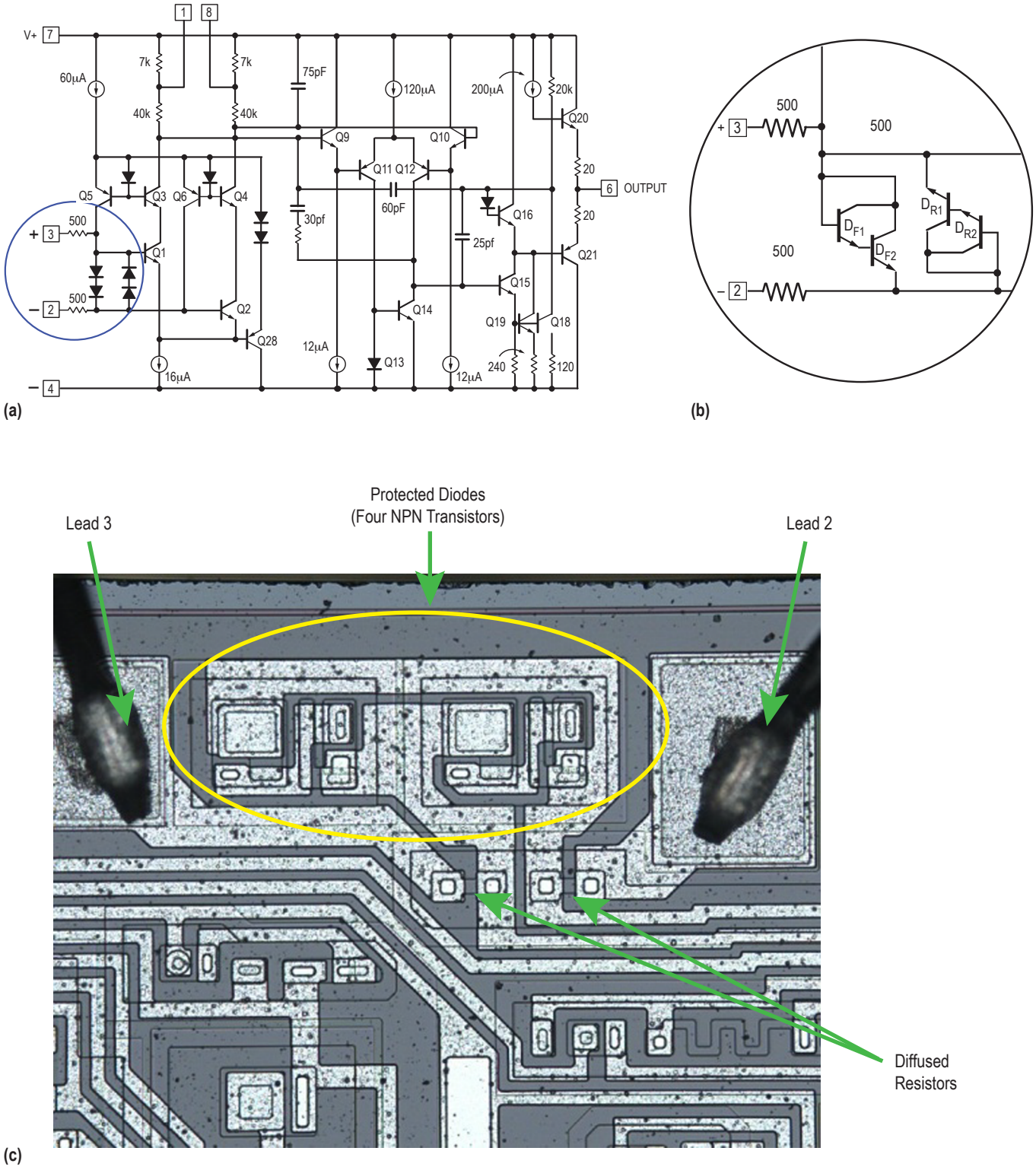

Figure 7. Schematic drawings of (a) the op amp circuit and (b) the base-emitter junctions of four transistors used as the protective diodes. Locations of the leads, diffused resistors, and protected ‘diodes’ on a known good op amp die are shown in (c).

Table 2. Pulses applied to op amps.

Sample Number	Pulse Properties			
	Voltage (V)	Pulse Width (µs)	Energy (µJ)	Current (A)
Damage caused change in resistance to diffused resistors (refer to figure 8(a))				
18	70	4.5	365.0	11.40
19	80	3.0	340.0	13.00
25	100	1.5	152.0	12.70
30	–100	1.0	96.3	5.85
33	–90	1.5	119.3	10.50
37	–70	4.0	117.0	5.18
38	–70	5.0	381.0	11.75
42	–60	10.0	340.0	9.54
44	–60	10.5	524.0	10.25
Damage caused change in breakdown voltages (refer to figure 8(b))				
9	60	6.0	118	3.98
12	60	6.5	317	9.90
15	60	7.0	392	9.85
13	60	7.5	401	9.90
16	70	4.0	272	10.00
18	70	4.5	364	11.40
22	90	2.0	212	12.80
35	–80	2.5	226	11.30
36*	–80	2.8	313	13.47
Damage caused electrical open (refer to figure 8(c))				
14	60	8.0	924	5.05
17	70	5.0	619	11.30
21	80	3.5	599	13.00
20	80	4.0	790	6.30
24	90	2.5	522	13.90
23	90	3.0	889	14.20
26	100	1.8	373	15.10
7	100	2.0	650	15.10
29	–100	1.5	537	16.10
28	–100	1.8	705	11.60
32	–90	2.0	512	14.80
31	–90	3.0	1,140	9.60
34	–80	3.0	519	13.55
39	–70	5.5	548	11.80
45	–60	11.0	594	10.35

* Junctions were shorted, resulting in the resistive curve shown in figure 11(b).

Curve traces and an optical image of op amp sample 33 are shown figure 8, which is a typical sample exhibiting the first characteristic. The sample received a –90-V, 1.5-µs pulse and had a resulting energy of 119.3 µJ. Figures 8(a) and 8(b) show curve traces of the device before the pulse was applied and after the pulse was applied, respectively. Note the increased slopes of the lines, which indicate a decrease in resistance. Figure 8 (c) is an image of the damage site using a bright field objective with × 50 magnification. The yellow arrows mark the damaged resistors.

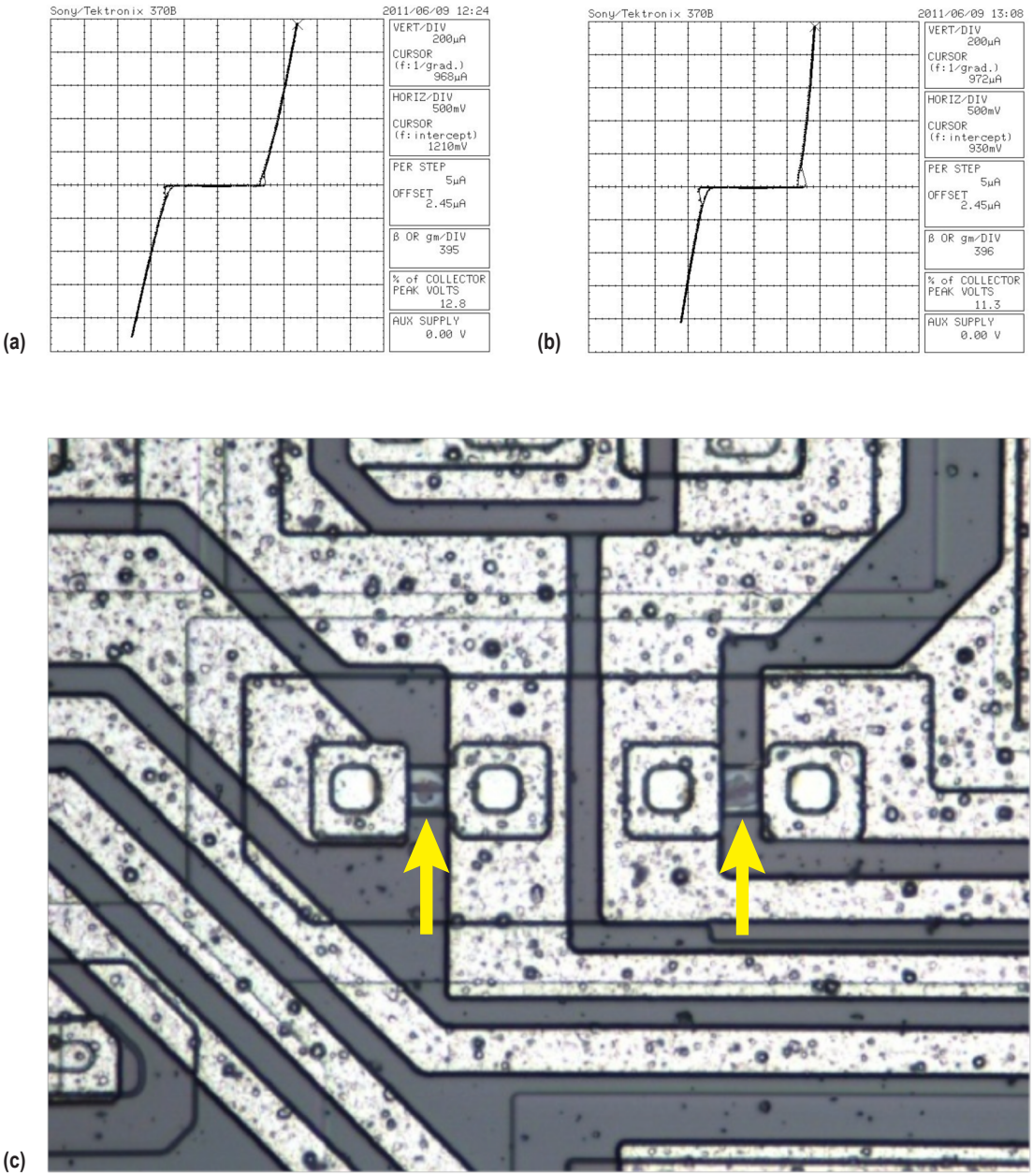

Figure 8. Op amp sample 33: Curve traces of (a) the device before the pulse was applied, (b) the device after the pulse was applied, and (c) an image of the damage site using a bright field objective with × 50 magnification.

The second characteristic noted was similar damage to the diffused resistors as in the first characteristic and an increase in the forward breakdown voltage from 750 mV to approximately 1 V, regardless of the polarity of the pulse applied (see figs. 9 and 10).

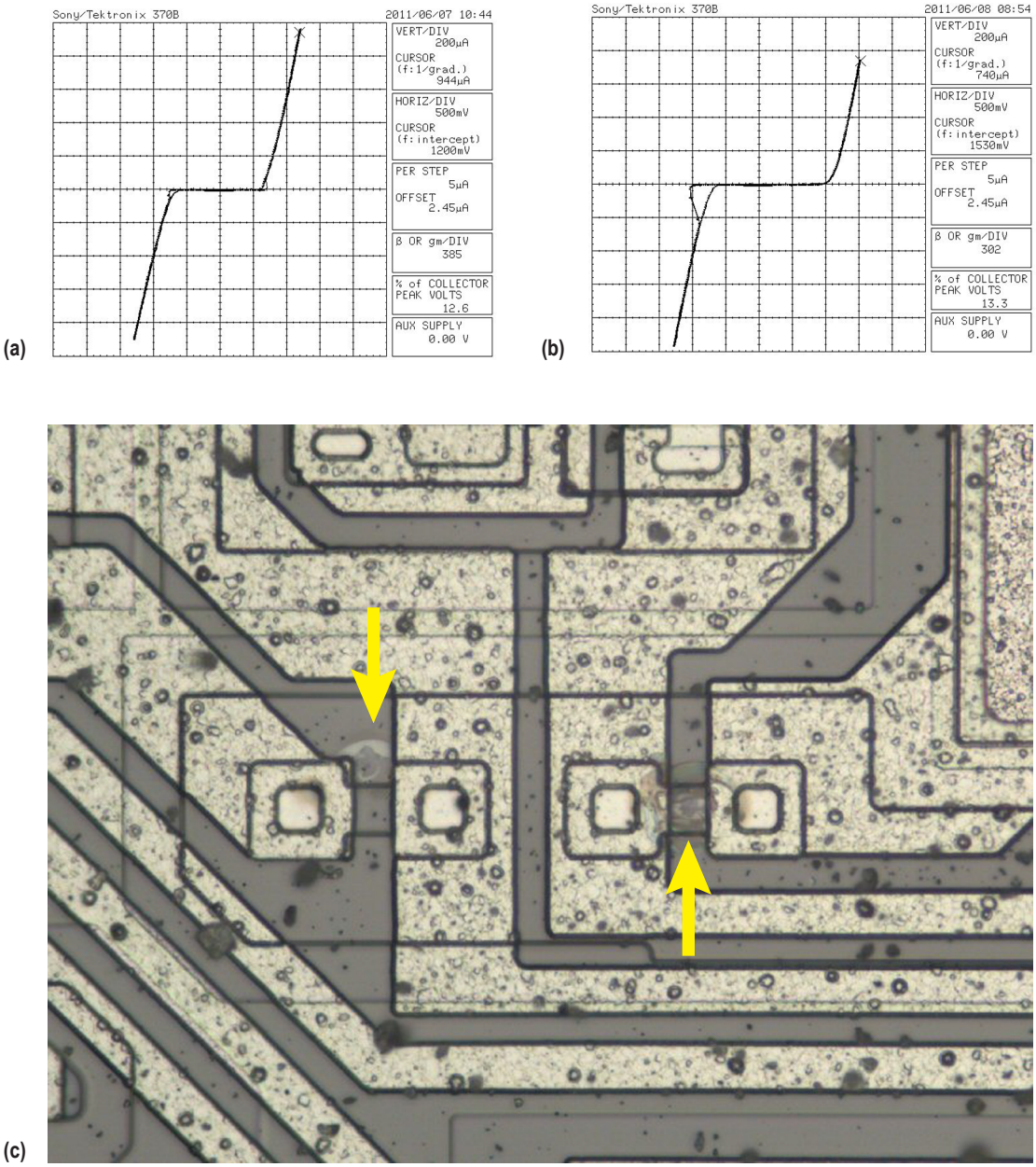

Figure 9. Op amp sample 16: Curve traces of (a) the device before the pulse was applied, (b) the device after the pulse was applied, and (c) an image of the damage site using a bright field objective with × 50 magnification.

Curve traces and an optical image of op amp sample 16 are shown in figure 9. The sample received a 70-V, 4-µs pulse and had a resulting energy of 272 µJ. Figures 9(a) and 9(b) depict curve traces of the device before the pulse was applied and after the pulse was applied, respectively. Figure 9(c) is an image of the damage site using a bright field objective with × 50 magnification. The damage sites (yellow arrows) are similar to those shown in figure 8(c). However, a few differences are noted. The forward breakdown voltage increased from 750 mV to approximately 1 V, the breakdowns have 'soft knees,' and the hysteresis at the negative breakdown is more pronounced.

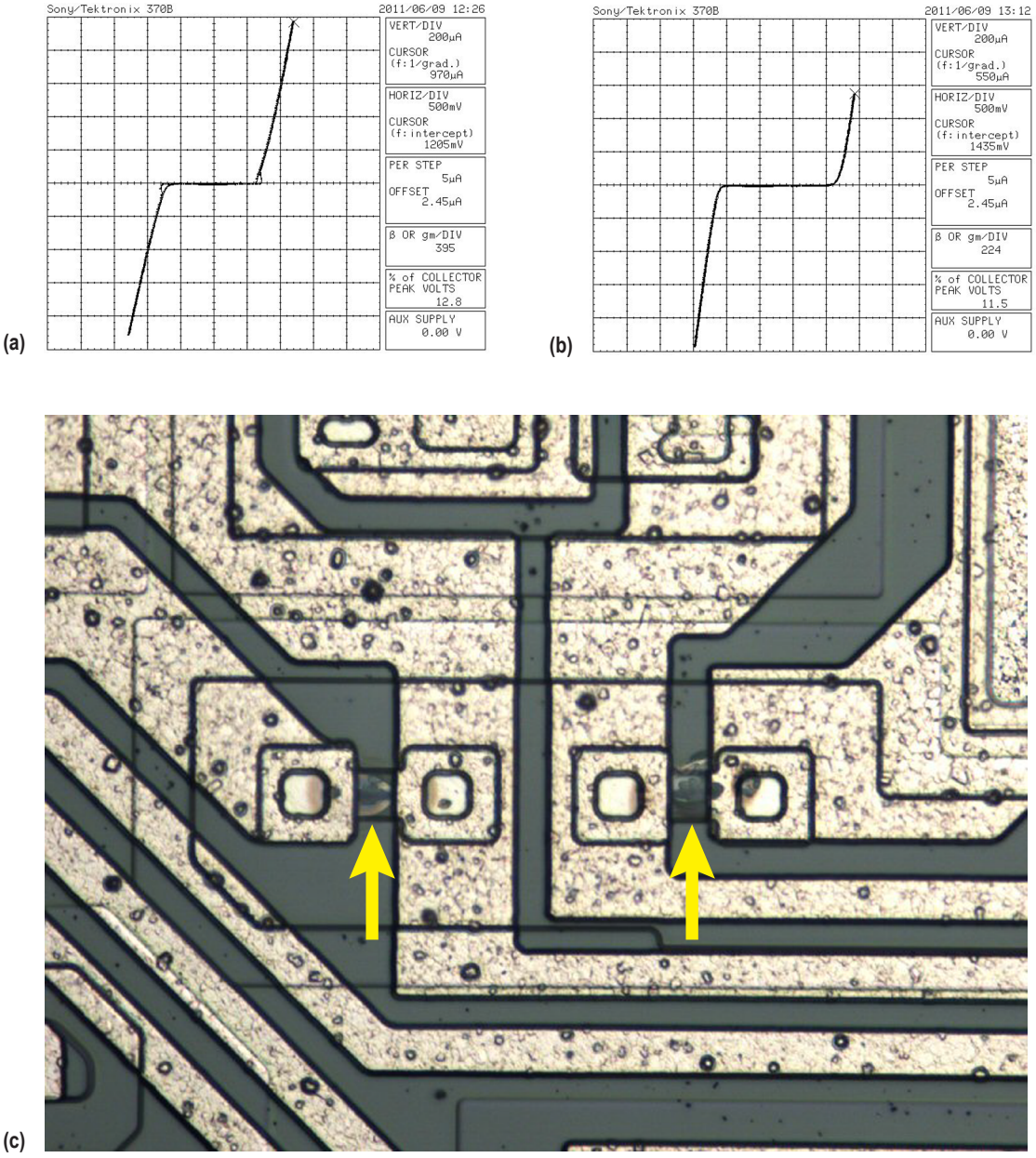

Figure 10. Op amp sample 35: Curve traces of (a) the device before the pulse was applied, (b) the device after the pulse was applied, and (c) an image of the damage site using a bright field objective with × 50 magnification.

Curve traces and an optical image of op amp sample 35 are shown in figure 10. The sample received a –80-V, 2.5-μs pulse and had a resulting energy of 226 μJ. Figures 10(a) and 10(b) depict curve traces of the device before the pulse was applied and after the pulse was applied, respectively. Figure 10(c) is an image of the damage site using a bright field objective with × 50 magnification. The damage sites (yellow arrows) are similar to those shown for sample 16 in figure 9(c).

'Soft-knee' breakdowns and increased hysteresis were also found in other examples. In one case, the lateral transistors were shorted, resulting in a 1,000-Ω resistive curve trace. Curve traces and an optical image of op amp sample 36 are shown in figure 11. The sample received a –80-V, 2.8-μs pulse and had a resulting energy of 313 μJ. Figures 11(a) and 11(b) show the curve trace of the device before the pulse was applied and after the pulse was applied, respectively. This indicates that some damage occurred in the lateral NPN transistor junctions; however, no physical damage was observed on the die in the transistor area using optical microscopy. Figure 11(c) is an image of the damage site using a bright field objective with × 20 magnification. The damage to the diffused resistors (yellow arrows) is similar to the resistor damage of sample 16 shown in figure 10(c). An area of heat damage and discoloration of an aluminum trace at one of the resistor contact vias was also noted (blue arrow), which is typical damage observed on samples subjected to energies greater than 300 μJ.

For the first two characteristics, pulses applied having energies between 300 and 400 μJ began to show heat damage and discoloration of aluminum traces in addition to the melt through at 401 μJ. Curve traces and an optical image of sample 13 are shown in figure 12. The sample received a 60-V, 7.5-μs pulse and had a resulting energy of 401 μJ. Figures 12 (a) and 12(b) show the curve traces of the device before the pulse was applied and after the pulse was applied, respectively. Note the increased slopes of the lines, which indicate a decrease in resistance. In addition, the forward breakdown voltage increased from 750 mV to approximately 1 V, and increase hysteresis is observed at the negative breakdown. Figure 12(c) is an image of the damage site using a bright field objective with × 50 magnification. Both resistors have been damaged. The yellow arrows mark areas suffering heat damage and discoloration.

The third characteristic of damage was an open circuit. Pulses having energies exceeding 500 μJ showed splattering, metal flow, and significant damage to the glassivation, which is typical. Curve traces and an optical image of op amp sample 23 are shown in figure 13. The sample received a 90-V, 3-μs pulse and had a resulting energy of 889 μJ. The size of the damage area appeared to grow and sometimes included damage to the two forward bias protected diodes as the pulse width and voltage were increased. Figures 13(a) and 13(b) show curve traces of the device before the pulse was applied and after the pulse was applied, respectively. Figure 13(b) indicates the device is electrically open between pins 3 and 2. Figure 13(c) is an image of the damage site using a bright field objective with × 20 magnification. The yellow circle shows an area of heat damage where the metal is discolored. The yellow arrows mark where the aluminum traces were melted and splattered to the surrounding area. Significant damage to the glassivation also occurred.

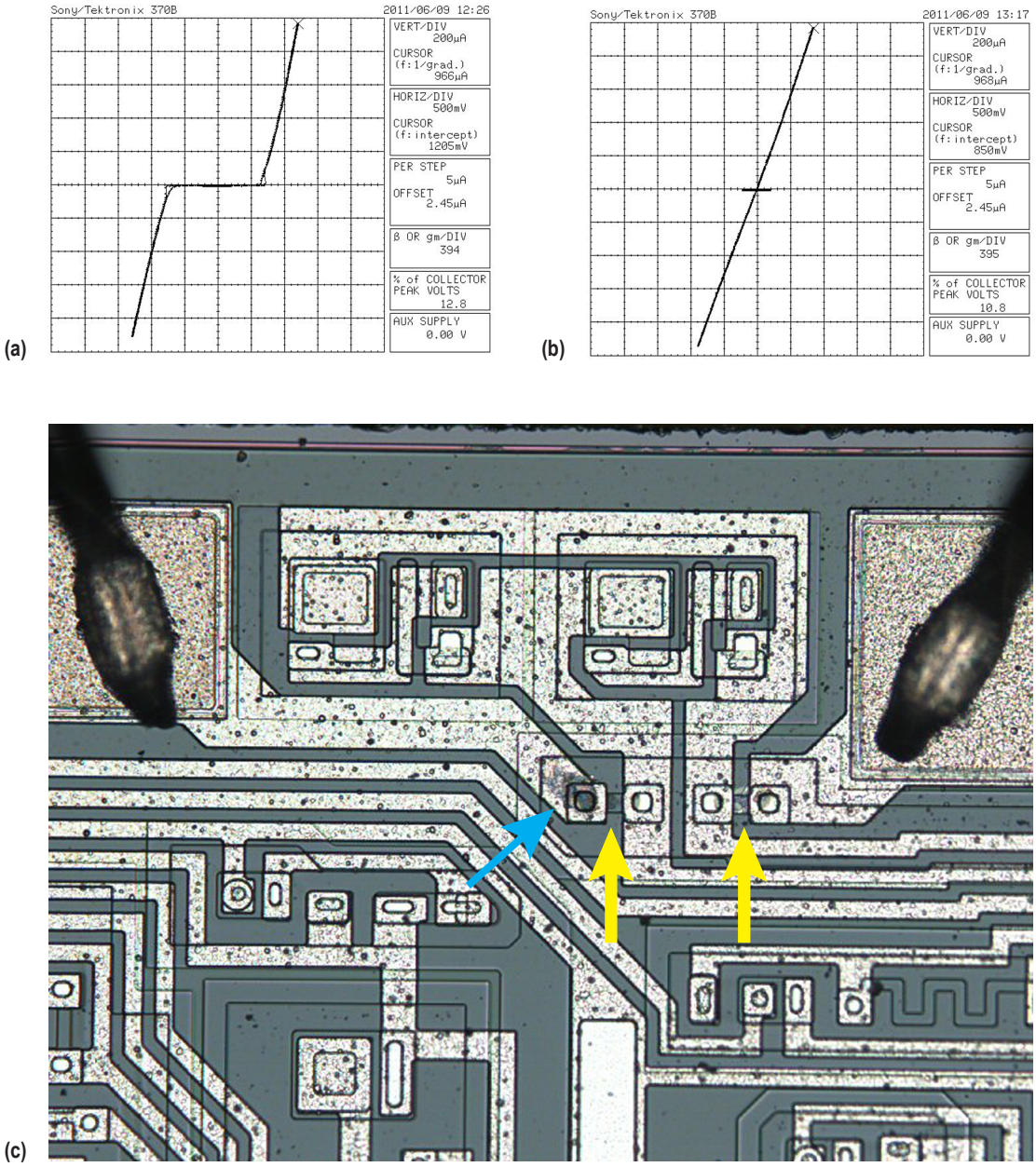

Figure 11. Op amp sample 36: Curve traces of (a) the device before the pulse was applied, (b) the device after the pulse was applied, and (c) an image of the damage site using a bright field objective with × 20 magnification.

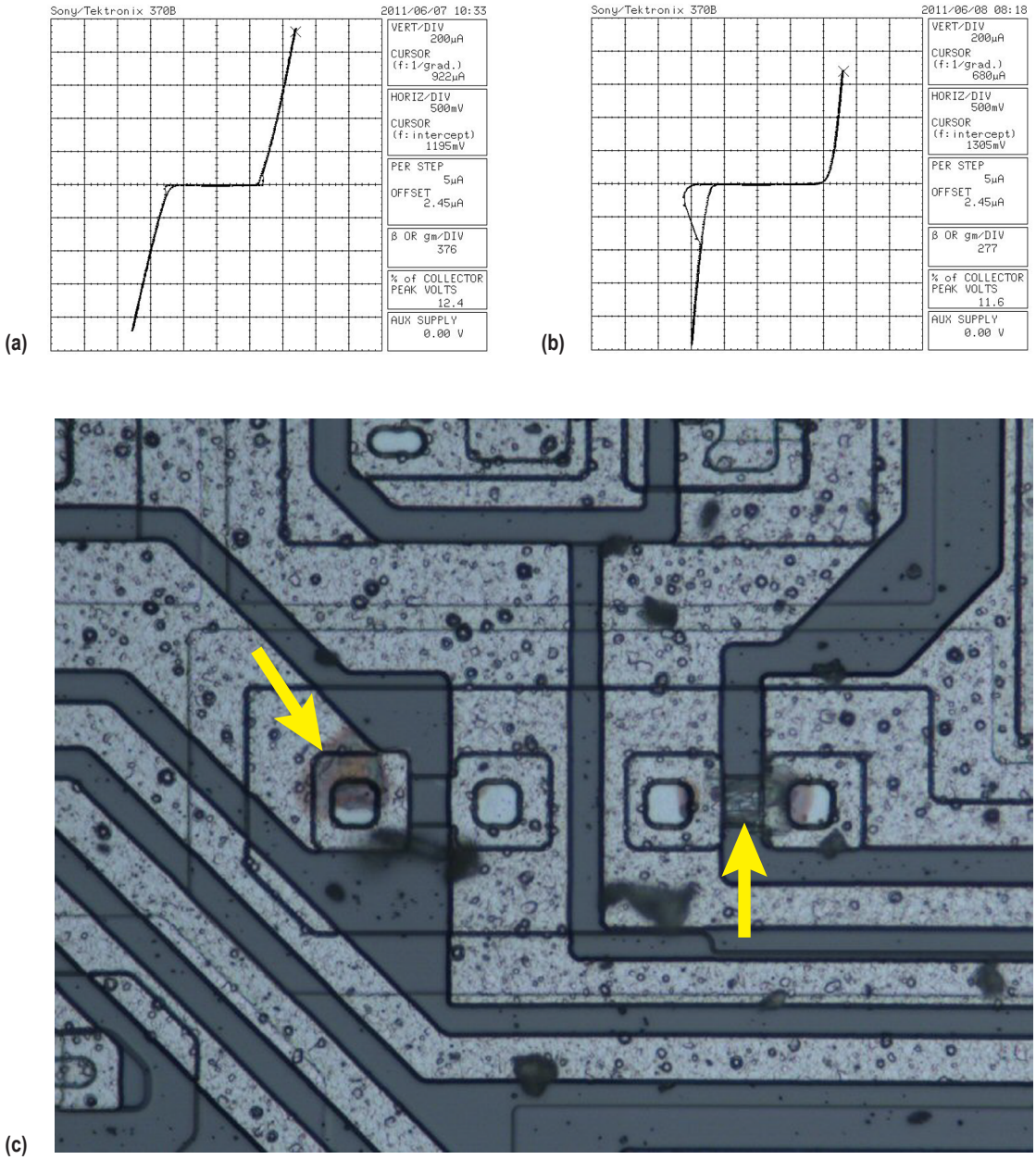

Figure 12. Op amp sample 13: Curve traces of (a) the device before the pulse was applied, (b) the device after the pulse was applied, and (c) an image of the damage site using a bright field objective with × 50 magnification.

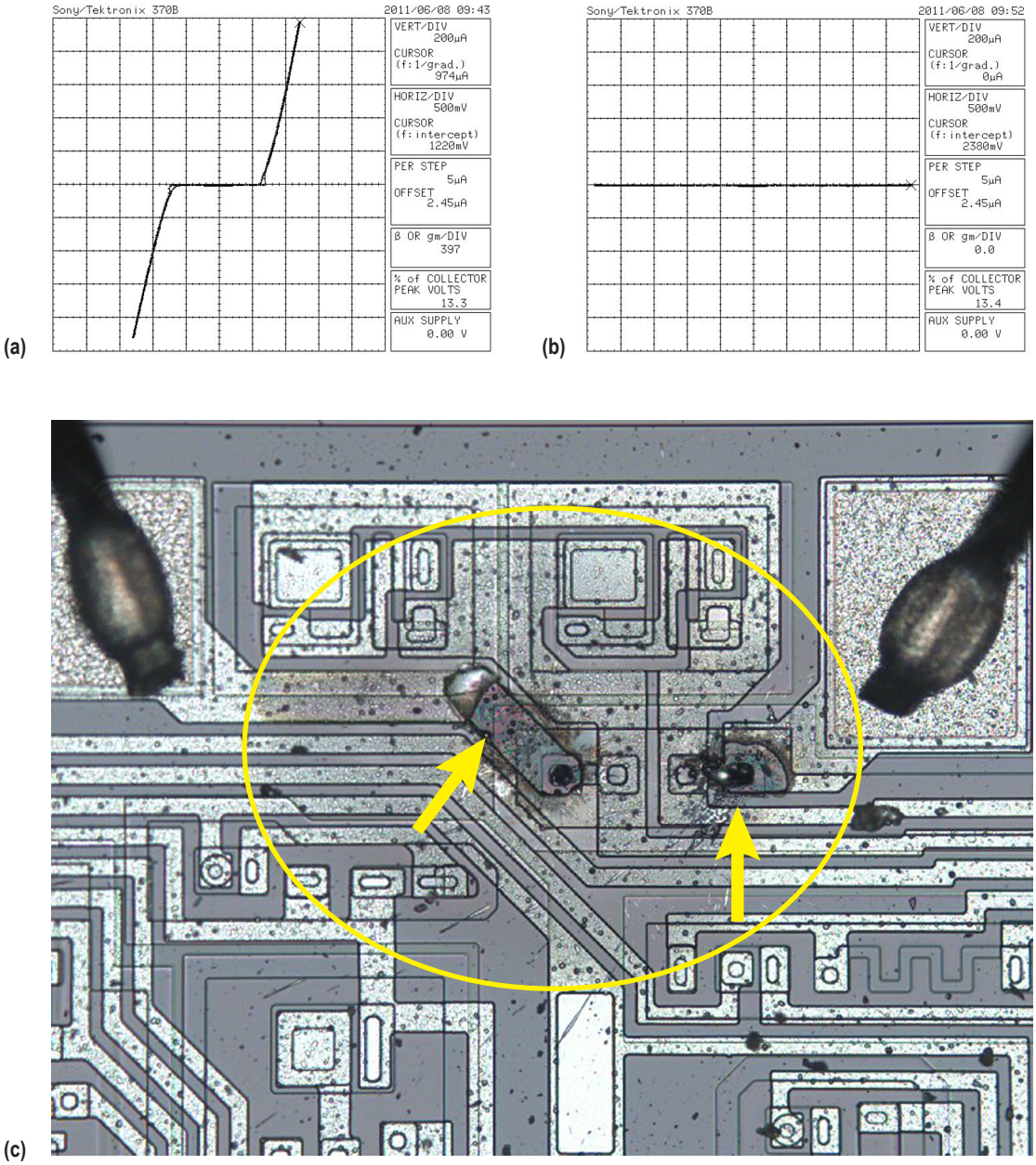

Figure 13. Op amp sample 23: Curve traces of (a) the device before the pulse was applied, (b) the device after the pulse was applied, and (c) an image of the damage site using a bright field objective with × 20 magnification.

Figure 14 demonstrates how damage caused by positive and negative pulses was very similar. Curve traces and an optical image of op amp sample 32 are shown. The sample received a –90-V, 2-µs pulse and had a resulting energy of 513 µJ. Figures 14(a) and 14(b) show curve traces of the device before the pulse was applied and after the pulse was applied, respectively. Figure 14(b) indicates the device is electrically open between pins 3 and 2. Figure 14(c) is an image of the damage site using a bright field objective with × 20 magnification. The damage observed is similar to the damage to sample 23 shown in figure 13.

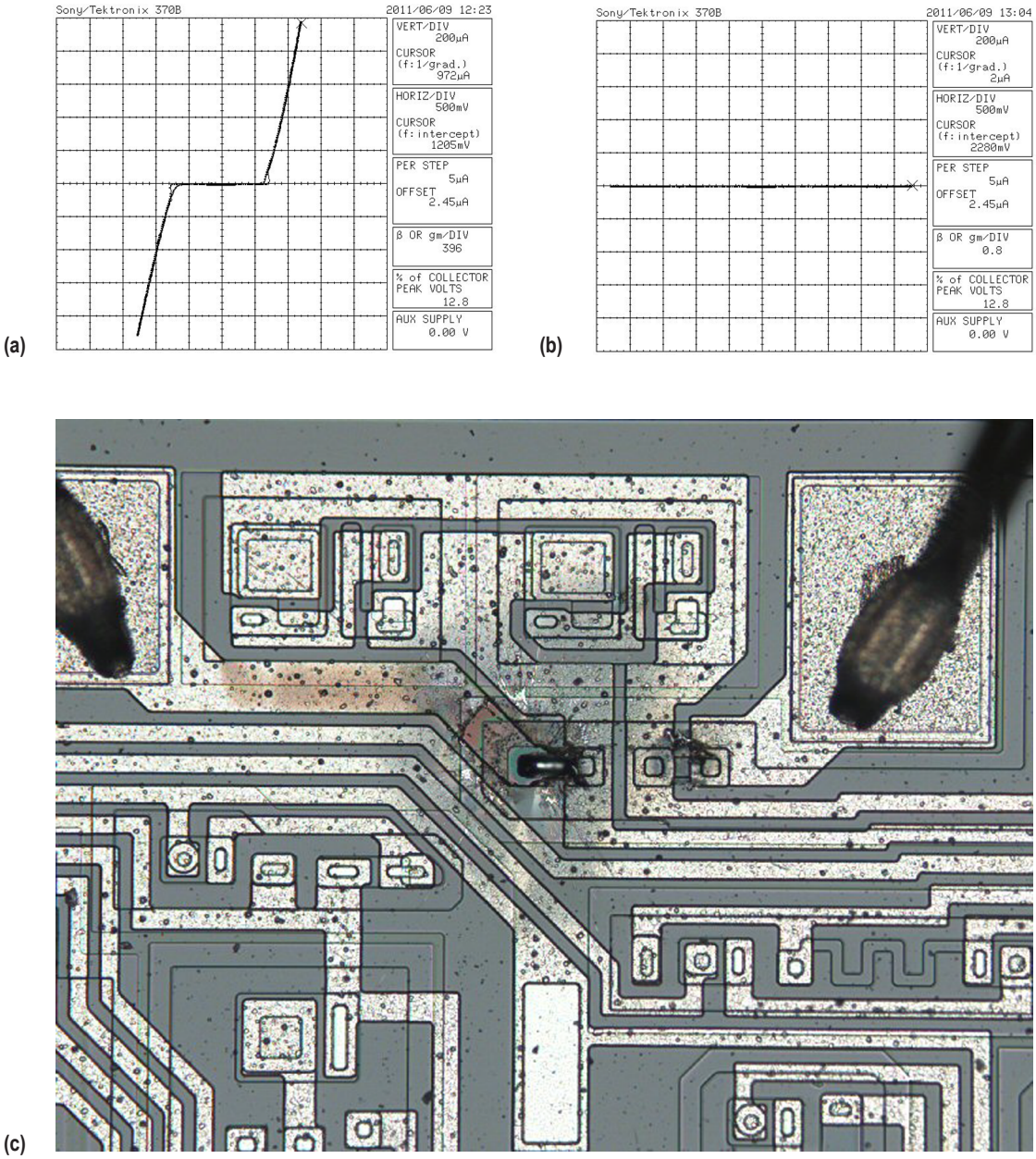

Figure 14. Op amp sample 32: Curve traces of (a) the device before the pulse was applied, (b) the device after the pulse was applied, and (c) an image of the damage site using a bright field objective with × 20 magnification.

In a few instances, there were overlaps in the exact amount of energy needed to severely, moderately, or slightly damage each part. Although parts were chosen to be as similar as possible, each part has a slightly different breakdown voltage, which contributes to its ability to withstand the pulse applied to it. Also, constant voltages could not be maintained over the duration of the pulse in some cases because of current limitations associated with the pulse generator. This caused unpredictable variations in the pulses applied to each part, which contributed to the deviations in damage observed.

4.2 Transistors

The pulse width, current, energy, and voltage supplied to the transistors were recorded using an oscilloscope. These values are listed in the Pulse Properties columns in table 3 for the reverse bias conditions and table 4 for the forward bias conditions.

Table 3. Pulses applied to reverse bias transistors.

Reverse Bias Emitter to Base					
	Pulse Properties				
Sample Number	Voltage (V)	Pulse Width	Energy (µJ)	Current (A)	Result of Damage
2	50	1µs	188.0	6.52	Reduced gain
1	55	1µs	205.0	7.20	β-characteristic reduced to diode curves
3	60	1µs	225.0	8.00	(No curve trace)
8	200	1µs	355.0	17.30	β-characteristic reduced to diode curve
7	250	1µs	165.0	18.60	Resistive short of 55 Ω
4	100	250ns	96.5	7.80	β-characteristic reduced to diode curves
5	200	250ns	174.0	19.60	Resistive short of 191 Ω
6	300	250ns	171.0	20.00	Resistive short of 422 Ω
Reverse Bias Collector to Base					
	Pulse Properties				
Sample Number	Voltage (V)	Pulse Width	Energy (µJ)	Current (A)	Result of Damage
23	80	8µs	2,990	17.70	Resistive short of 3.3 Ω
21	90	8µs	637	8.50	Resistive short of 5.7 Ω
20	85	5µs	2,220	18.20	Resistive short of 2.8 Ω
18	90	5µs	656	16.70	Resistive short of 9.6 Ω
13	150	1µs	426	15.50	Resistive short of 28.6 Ω
12	150	2µs	471	19.90	Resistive short of 16.5 Ω
10	200	200ns	207	8.60	β-characteristic reduced to diode curve
11	200	600ns	343	14.60	β-characteristic reduced to diode curves
16	300	100ns	160	17.00	β-characteristic reduced to diode curve
14	300	200ns	377	21.20	β-characteristic reduced to diode curves
Reverse Bias Collector to Emitter					
	Pulse Properties				
Sample Number	Voltage (V)	Pulse Width (µs)	Energy (µJ)	Current (A)	Result of Damage
37	100	1	56.2	19.00	No damage
39	110	1	230.0	9.60	Resistive short of 37.6 Ω
38	120	1	332.0	14.00	Resistive short of 8.2 Ω
40	130	1	245.0	10.56	Resistive short of 24.9 Ω
41	140	1	280.0	19.90	Resistive short of 15.8 Ω
42	150	1	243.0	11.52	Resistive short of 180.4 Ω
43	200	1	241.0	15.60	Resistive short of 118.6 Ω

Table 4. Pulses applied to forward bias transistors.

Forward Bias Emitter to Base					
	Pulse Properties				
Sample Number	Voltage (V)	Pulse Width (µs)	Energy (mJ)	Current (A)	Result of Damage
55	50	15	1.75	13.38	No damage
54	50	20	2.59	13.29	Resistive short of 1,010 Ω
53	50	25	3.15	13.32	Resistive short of 1,004 Ω
52	50	30	3.96	13.32	Resistive short of 82.4 Ω
51	50	35	4.51	12.66	Resistive short of 9.6 Ω
47	50	40	4.87	12.87	Resistive short of 2.8 Ω
50	45	40	4.25	12.57	β-characteristic reduced to diode curves
49	40	40	3.24	11.58	No damage
48	40	30	2.61	11.50	No damage
44	40	100	8.15	8.61	Resistive short of 6.8 Ω
Forward Bias Collector to Base					
	Pulse Properties				
Sample Number	Voltage (V)	Pulse Width (µs)	Energy (mJ)	Current (A)	Result of Damage
59	40	40	3.17	11.52	No damage
58	45	40	3.73	12.66	β-characteristic reduced to diode curves
56	50	40	4.78	13.44	Base-collector shorted
57	55	40	7.13	14.28	β-characteristic reduced to diode curve
60	60	40	7.98	15.00	β-characteristic reduced to diode curve
66	50	25	2.89	13.38	No damage
65	50	30	3.34	13.59	β-characteristic reduced to diode curves
64	50	35	4.06	13.56	β-characteristic reduced to diode curves
62	50	45	5.73	13.26	β-characteristic reduced to diode curve
63	50	50	6.49	13.26	Resistive short of 3.8 Ω
Forward Bias Collector to Emitter					
	Pulse Properties				
Sample Number	Voltage (V)	Pulse Width (µs)	Energy (µJ)	Current (A)	Result of Damage
32	40	1	114	8.40	Reduced β
33	50	1	162	10.95	Reduced β
34	60	1	215	13.44	Resistive short*
31	80	1	213	8.70	Resistive short of 360 Ω
36	100	1	132	14.72	No damage
24	30	8	665	6.08	Resistive short of 4.8 Ω
25	40	8	928	10.28	Resistive short of 6.3 Ω
26	50	8	1,180	12.70	Resistive short of 8.9 Ω
27	60	8	1,470	14.80	Resistive short of 4.3 Ω
28	70	8	1,730	16.50	Resistive short of 4.4 Ω
30	80	8	181	16.70	Reduced β
29	100	8	133	18.20	Reduced β

* Value of resistive short not measured.

4.2.1 Reverse Bias Emitter to Base

The damage observed in the samples that were pulsed reverse bias emitter to base (positive on the base and negative on the emitter) always originated on the smallest radius bends of the emitter-base junction nearest the emitter pad. This is expected because the first area to turn on in a transistor is usually the fingers nearest the emitter or base pads.[4] In addition, the junction geometry in these areas creates the highest electric fields found on an active transistor. Energy pulses as low as 174 μJ were capable of causing a resistive short through the base-emitter-collector junctions (see fig. 15) or causing a resistive short through the collector-base junction (see fig. 16).

Figure 15(a) is an image of transistor sample 5 using a bright field objective with × 20 magnification. The sample received a 200-V, 250-ns pulse that had a resultant energy of 174 μJ. The yellow arrow points to the damaged area. Figure 15(b) shows the transistor β characteristic curve trace that resulted from the emitter-base-collector being shorted, which indicates an emitter-base-collector resistive short of 191 Ω. Figure 16(a) is an image of transistor sample 4 using a bright field objective with × 20 magnification. The sample received a 100-V, 250-ns pulse that had a resultant energy of 96.5 μJ. The yellow arrow points to the damaged area. Figure 16(b) shows the collector-base curve trace obtained after the pulse was applied, which indicates a resistive short through the junction. Figure 16(c) shows that the curve trace of the base-emitter junction is nominal. Figure 16(d) shows the collector-emitter confirming the resistive short through the collector-base junction. The typical collector-emitter breakdown voltage of this device type is specified as a minimum of 60 V. The curve trace shows a breakdown voltage of 0.75 V.

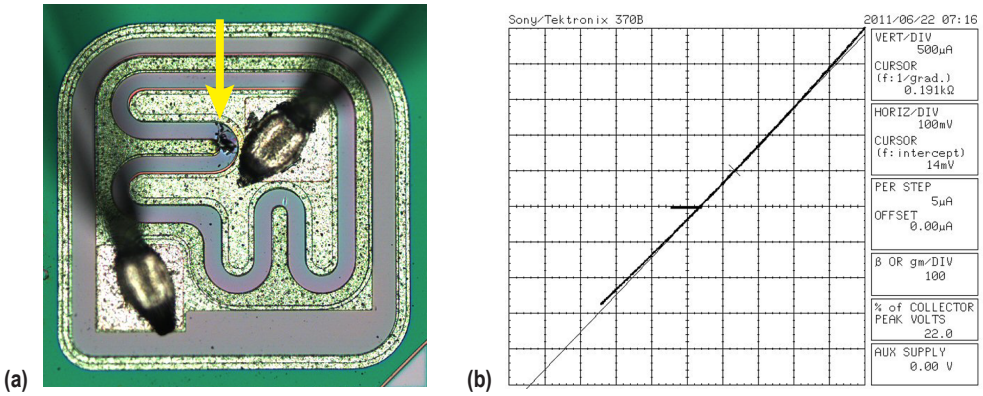

Figure 15. An image of (a) transistor sample 5 using a bright field objective with × 20 magnification, and (b) the transistor β characteristic curve trace that resulted from the emitter-base-collector being shorted.

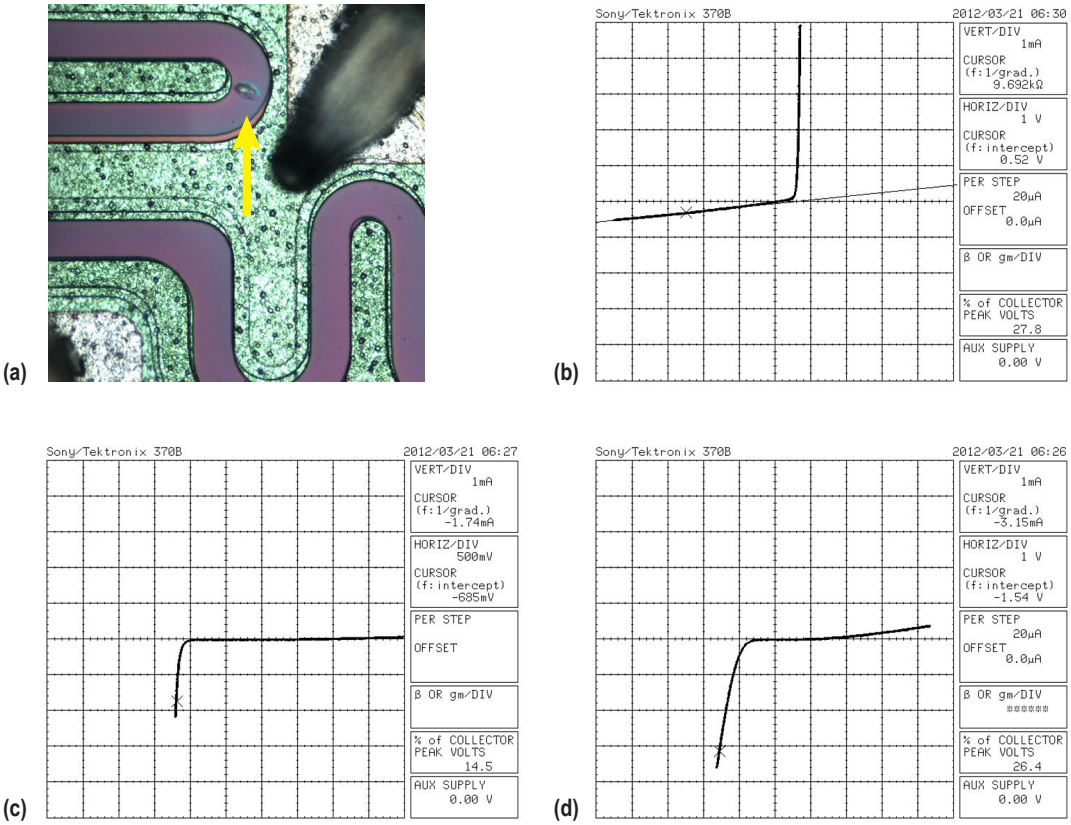

Figure 16. An image of (a) transistor sample 4 using a bright field objective with × 20 magnification, (b) the collector-base curve trace obtained after the pulse was applied, (c) a curve trace showing that the base-emitter junction is nominal, and (d) the collector emitter curve trace obtained confirming the resistive short through the collector-base junction.

4.2.2 Reverse Bias Collector to Base

The transistors that were pulsed reverse bias collector to base (positive on the base and negative on the collector) again showed damage in the small radius bends of the emitter-base junction, which resulted in low-resistive shorts; however, in this case the prominent damage occurs in the base region of the extended emitter fingers. The resultant visible damage is dependent on the amount of time it takes for the junction to break down. The longer it takes for the junction to break down, the more damage that will be accrued. The amount of time it takes for any particular junction to break down depends on the part's original breakdown voltage and the amount of pulse energy applied to it. The two transistors in figures 17 and 18 demonstrate this point. The transistor that was pulsed with the lower voltage had more extensive damage due to the increased breakdown time. This is caused when the pulse generator stops the supply of voltage after junction breakdown.

An image of transistor sample 23 using a bright field objective with × 20 magnification is shown in figure 17(a). The sample received an 80-V, 8-µs pulse that had a resultant energy of 2,990 µJ. Figure 17(b)shows the transistor β characteristic curve trace that resulted from the emitter-base-

collector being shorted, which indicates a 3.3-Ω resistive short. An image of transistor sample 21 using a bright field objective with × 20 magnification is shown in figure 18(a). The sample received a 90-V, 8-µs pulse that had a resultant energy of 637 µJ. Figure 18(b) shows the transistor β characteristic curve trace that resulted from the emitter-base-collector being shorted, which indicates a 5.7-Ω resistive short. Damage areas are marked with yellow arrows.

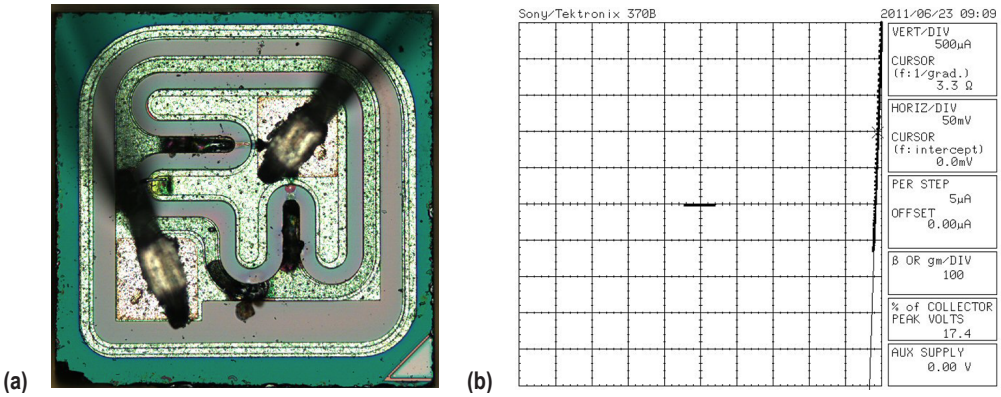

Figure 17. An image of (a) transistor sample 23 using a bright field objective with × 20 magnification, and (b) the transistor β characteristic curve trace that resulted from the emitter-base-collector being shorted.

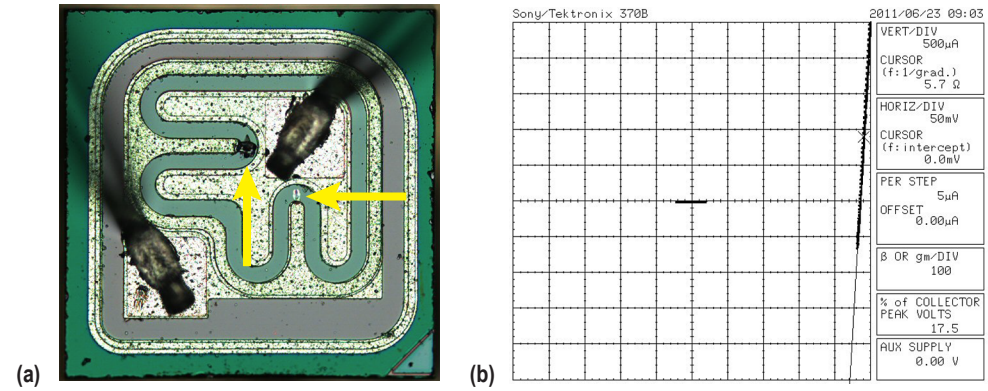

Figure 18. An image of (a) transistor sample 21 using a bright field objective with × 20 magnification, and (b) the transistor β characteristic curve trace that resulted from the emitter-base-collector being shorted.

4.2.3 Reverse Bias Collector to Emitter

For the samples pulsed in this orientation (positive on the emitter and negative on the collector), the metallograph showed no visible damage even though the curve tracer indicated that there was a resistive short in all samples except sample 37 (see table 3), which was not damaged. This is because the damage is most likely located under the emitter lead and extends straight

down to contact with the collector. To verify this, cross sectioning would have to be performed. Cross-sectional analysis is beyond the scope of this study but will be a focus of future work. Figure 19(a) is an image of transistor sample 42 using a bright field objective with × 20 magnification, and figure 19(b) shows the transistor β characteristic curve trace that resulted from the emitter-base-collector being shorted, which indicates a 180.4-Ω resistive short.

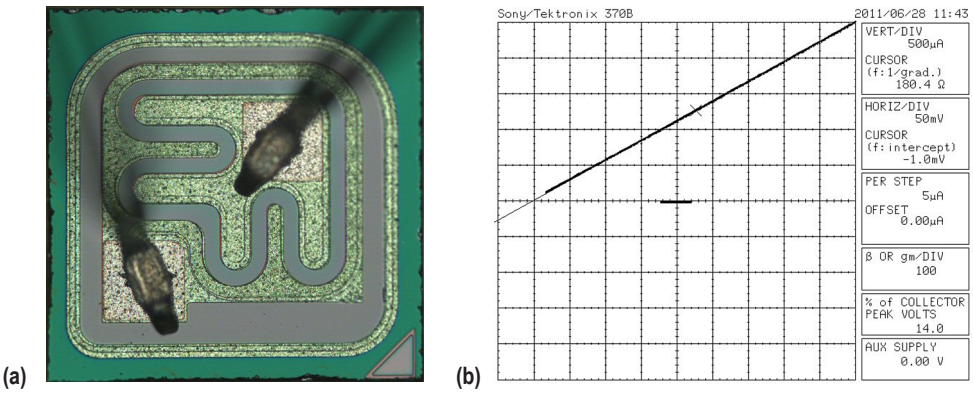

Figure 19. An image of (a) transistor sample 42 using a bright field objective with × 20 magnification, and (b) the transistor β characteristic curve trace that resulted from the emitter-base-collector being shorted.

4.2.4 Forward Bias Emitter to Base

The damage that occurs in samples that were pulsed forward bias emitter to base (positive on the emitter and negative on the base) begins at the critical bends of the emitter-base junction closest to the base pad. The relatively long pulse widths applied to these parts (20–40 µs in length) allowed melting of aluminum traces (see fig. 20). This type of damage is not possible with short pulses because it requires sufficient time to reach the temperatures needed to melt the aluminum (see fig. 21).

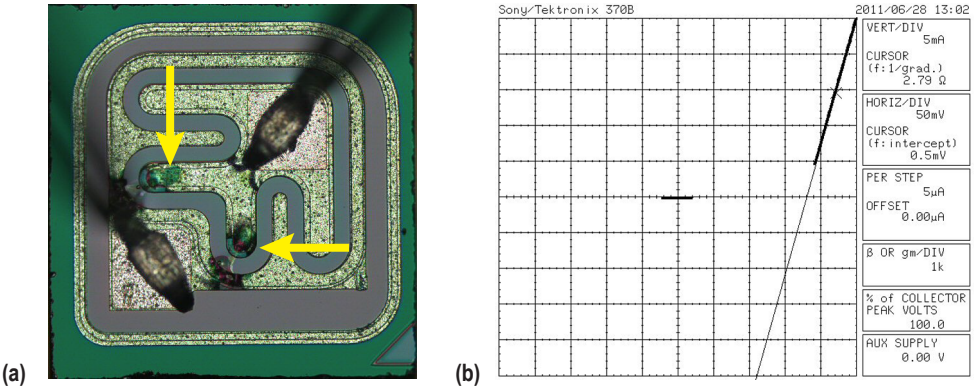

Figure 20. An image of (a) transistor sample 47 using a bright field objective with × 20 magnification, and (b) the transistor β characteristic curve trace that resulted from the emitter-base-collector being shorted.

An image of transistor sample 47 using a bright field objective with × 20 magnification is shown in figure 20(a). The sample received a 50-V, 40-µs pulse that had a resultant energy of 4.87 mJ. The yellow arrows mark the damaged areas. Figure 20(b) shows the transistor β characteristic curve trace that resulted from the emitter-base-collector being shorted, which indicates a 3-Ω resistive short. An image of transistor sample 54 using a bright field objective with × 20 magnification is shown in figure 21(a). The sample received a 50-V, 20-µs pulse that had a resultant energy of 2.59 mJ. The damaged area is marked with a yellow arrow. Figure 21(b) is a forward bias collector to base curve trace showing a 1,010-Ω resistive short with a diode breakdown at approximately 0.55 V.

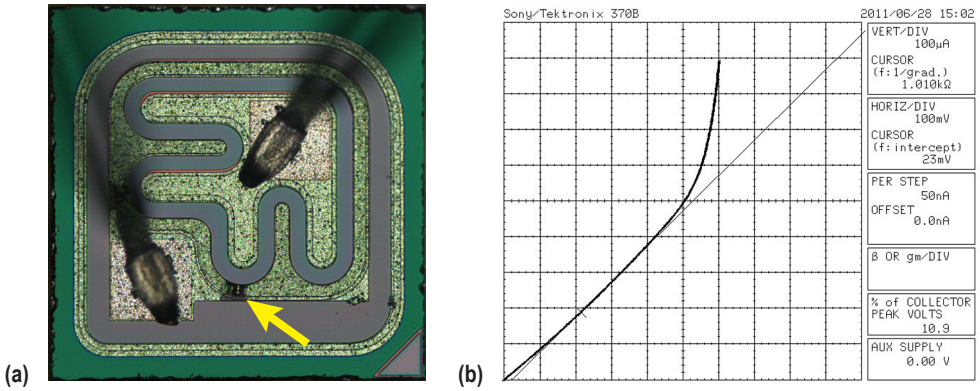

Figure 21. An image of (a) transistor sample 54 using a bright field objective with × 20 magnification, and (b) a forward bias collector to base curve trace showing a 1,010-Ω resistive short with a diode breakdown at approximately 0.55 V.

4.2.5 Forward Bias Collector to Base

The visible damage in the samples pulsed forward bias collector to base (positive on the collector and negative on the base) occurred in the base-collector junction region nearest the base pad. Samples subjected to pulses having energies <3.2 mJ were not damaged. Samples receiving pulse energies between 3.2 and 4.8 mJ suffered slight to moderate visual damage, which resulted in collector-base resistive shorts (see figs. 22 and 23).

An image of transistor sample 65 using a bright field objective with × 20 magnification is shown in figure 22(a). The sample received a 50-V, 30-µs pulse that had a resultant energy of 3.34 mJ. The collector-base curve trace obtained after the pulse was applied indicates a resistive short through the junction (see fig. 22(b)). Figure 22(c) shows that the curve trace of the base-emitter junction is nominal. The collector-emitter curve trace shown in figure 22(d) confirms the resistive short through the collector–base junction. The typical collector-emitter breakdown voltage of this device type is specified as a minimum of 60 V. The curve trace shows a breakdown voltage of 0.6 V.

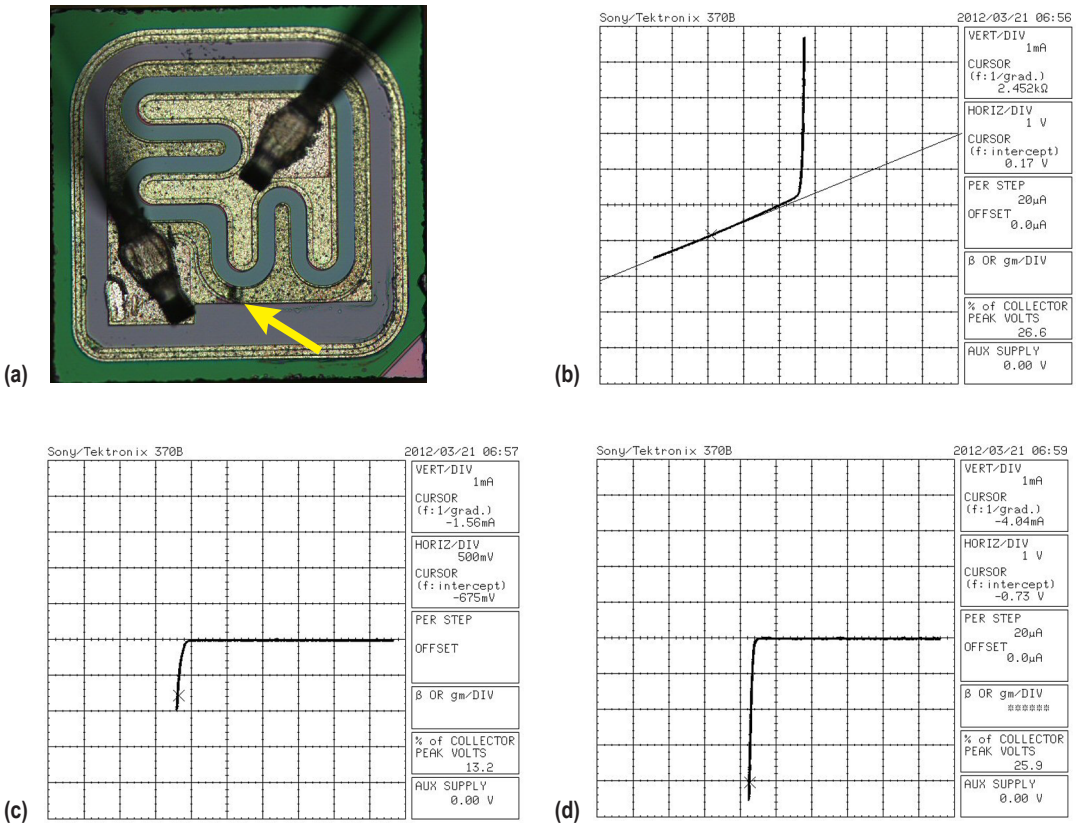

Figure 22. An image of (a) transistor sample 65 using a bright field objective with × 20 magnification, (b) the collector-base curve trace obtained after the pulse was applied, (c) a curve trace showing that the base-emitter junction is nominal, and (d) a collector-emitter curve trace that confirms the resistive short through the collector-base junction.

An image of transistor sample 56 using a bright field objective with × 20 magnification is shown in figure 23(a). The sample received a 50-V, 40-µs pulse that had a resultant energy of 4.78 mJ. Greater damage has occurred at the same location as in sample 65 (see fig. 22(a)). Figure 23(b) shows that the collector-base curve trace obtained after the pulse was applied and indicates a short through the junction. Figure 23(c) shows that the curve trace of the base-emitter junction is nominal. The collector-emitter curve trace shown in figure 23(d) confirms the resistive short through the collector-base junction. The typical collector-emitter breakdown voltage of this device type is specified as a minimum of 60 V. The curve trace shows a breakdown voltage of 0.6 V.

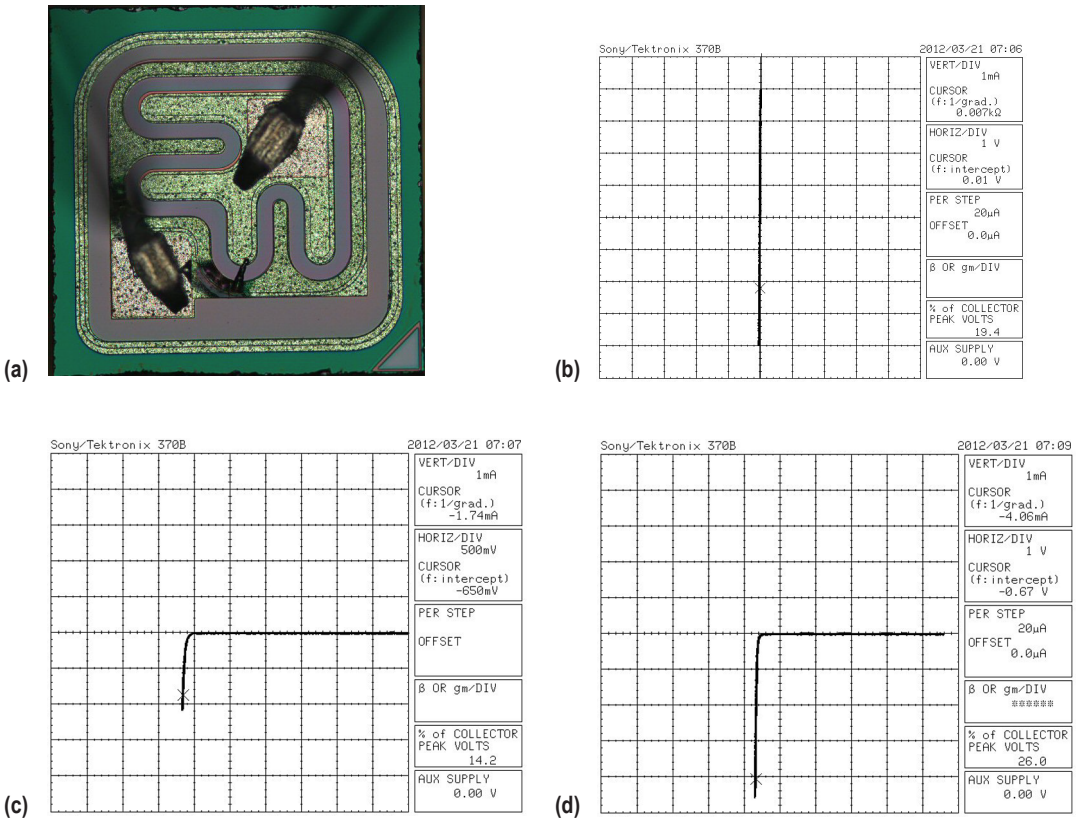

Figure 23. An image of (a) transistor sample 56 using a bright field objective with × 20 magnification, (b) the collector-base curve trace obtained after the pulse was applied, (c) a curve trace showing that the base-emitter junction is nominal, and (d) a collector-emitter curve trace that confirms the short through the collector-base junction.

Samples receiving pulses having energies >5.70 mJ sustained extensive melting of the aluminum and large amounts of damage to the base region. The base bond wire was actually fused in a couple of these samples, which sustained currents between 13 and 15 A for 25–30 μs (see fig. 24). An image of transistor sample 63 using a bright field objective with × 20 magnification is shown in figure 24(a). The sample received a 50-V, 50-μs pulse that had a resultant energy of 6.49 mJ. Major damage to the bond pad area has occurred and the base bond wire is fused open. The damaged area is marked by the yellow arrow. Figure 24(b) shows the transistor β characteristic curve trace that resulted from the emitter-base-collector being shorted.

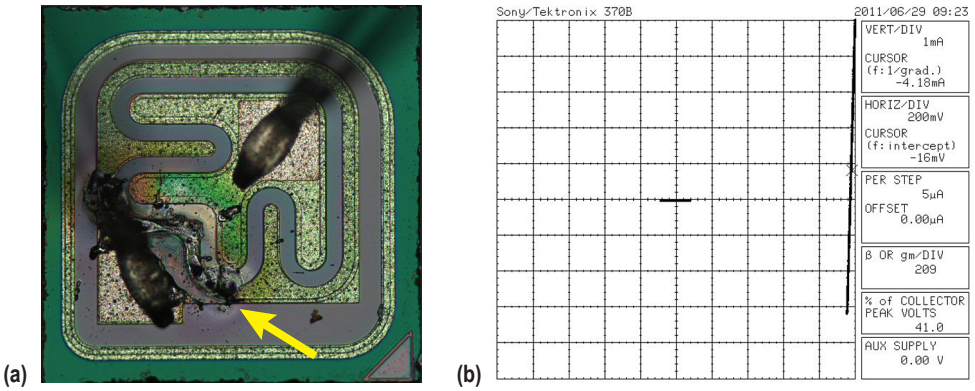

Figure 24. An image of (a) transistor sample 63 using a bright field objective with × 20 magnification, and (b) the transistor β characteristic curve trace that resulted from the emitter-base-collector being shorted.

4.2.6 Forward Bias Collector to Emitter

No visible damage was observed on samples pulsed forward bias collector to emitter (positive on the collector and negative on the emitter); however, the curve traces of some of the samples indicated there was extensive damage. Samples receiving pulses with energies <185 μJ were either not damaged or had reduced β (see fig. 25). An image of transistor sample 30 using a bright field objective with × 20 magnification is shown in figure 25(a). The sample received an 80-V, 8-μs pulse that had a resultant energy of 181 μJ. No physical damage was observed. Figure 25(b) is a characteristic set of curves that indicates the β was reduced from 185 to 144.

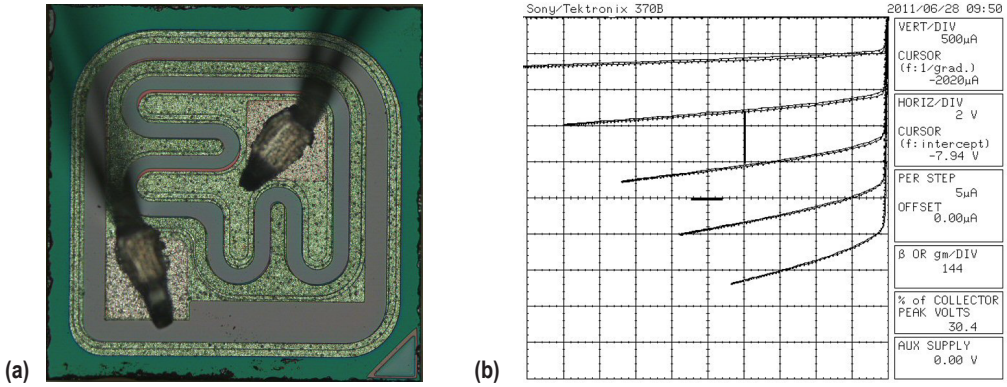

Figure 25. An image of (a) transistor sample 30 using a bright field objective with × 20 magnification, and (b) a characteristic set of curves that indicates the gain was reduced from 185 to 144.

Samples receiving pulses with energies from 185 µJ to 1.75 mJ resulted in resistive shorts (see fig. 26). The damage is probably located under the emitter pad. The resultant damage was an emitter-base-collector resistive short. These samples, along with the damaged samples that were pulsed reverse bias collector-emitter, will be investigated in future work. An image of transistor sample 27 using a bright field objective with × 20 magnification is shown in figure 26(a). The sample received a 60-V, 8-µs pulse that had a resultant energy of 1.47 mJ; however, no visible damage was observed. Figure 26(b)the transistor β characteristic curve trace that resulted from the emitter-base-collector being shorted, which indicates a resistive short of 4.3 Ω.

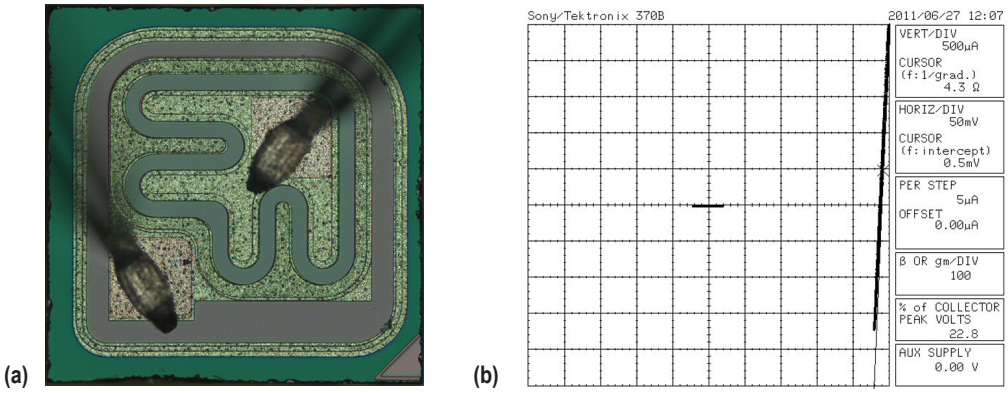

Figure 26. An image of (a) transistor sample 27 using a bright field objective with × 20 magnification, and (b) the transistor β characteristic curve trace that resulted from the emitter-base-collector being shorted.

5. CONCLUSION

The pulse width, voltage, and resultant energy all contribute to the damage inflicted to each part in a unique manner. However, it is difficult to differentiate exactly which combination of these parameters came together to create a damage site without a visual reference. After extensively examining the pictorial results from this study, there are several general trends to be noted. In a series of op amps that received a similar amount of energy as the voltage increased, the intensity of the heat damage also increased. In addition, for op amps pulsed with the same voltage and increasing pulse width, the initial splatter observed was the same, but the extent of burn-through increased with time. There is a range of energy for the op amps where the damage would randomly vary between change in resistance to diffused resistors and change in breakdown voltages. The data shows this energy range to be ≈115 to 400 μJ. Pulses having energies >500 μJ resulted in electrical opens.

The location of the transistor damage was dependent on the configuration of the pulse generator leads (whether forward or reverse bias emitter to base, collector to base, or collector to emitter) when each transistor was pulsed. Transistors do not turn on all at once. The first area to turn on is usually the fingers nearest the emitter or base pads, causing this to be the site for the majority of the damage. Another contributing factor is that the junction geometry in these areas creates high-electric fields. The damage remains in this area until these 'hot spots' start melting the components around them due to extensive pulse widths. In this study, some of the transistors' testing results were inconclusive due to the differences in the original breakdown voltages of each part. This can be avoided in the future by a more exhaustive prescreening of the transistors to be tested where the breakdown voltage variations are more tightly controlled.

This study is the beginning of a project to catalog a series of common EEE parts tested in this same manner. It is the intent of the catalog to provide the failure analyst with an intelligent starting point to begin this same analysis on devices similar to a failed NASA flight hardware component. This is done in hopes of recreating a damage site identical to the failed flight hardware component and providing invaluable information as to the source of the damage.

REFERENCES

1. Pierce, D.G; and Durgin, D.L.: "An Overview of Electrical Overstress Effects on Semiconductor Devices," *Proceeds of the 1981 EOS/ESD Symposium*, pp. 120–131, 1981.

2. Dicken, H.K.: *How to Analyze Failures of Semiconductors*, 2nd ed., pp. 130–151, DM Data Inc., Scottsdale, AZ, 1993.

3. Wait, J.V.; Huelsman, L.P.; and Korn, G.A.: *Introduction to Operational Amplifier Theory and Applications*, McGraw-Hill, NY, p. 2, 1975.

4. May, J.T.: "Limiting Phenomena in Power Transistors and the Interpretation of EOS Damage," *Microelectronic Failure Analysis: Desk Reference*, T.W. Lee and S.V. Pabbisetty (eds.), ASM International, Materials Park, OH, 3rd edition, pp. 169–175, 1993.

REPORT DOCUMENTATION PAGE

Form Approved
OMB No. 0704-0188

1. REPORT DATE *(DD-MM-YYYY)*	2. REPORT TYPE	3. DATES COVERED *(From - To)*
01–06–2012	Technical Memorandum	

4. TITLE AND SUBTITLE

Systematic Destruction of Electronic Parts for Aid in Electronic Failure Analysis

5a. CONTRACT NUMBER

5b. GRANT NUMBER

5c. PROGRAM ELEMENT NUMBER

6. AUTHOR(S)

S.E. Decker, T.D. Rolin, and P.D. McManus

5d. PROJECT NUMBER

5e. TASK NUMBER

5f. WORK UNIT NUMBER

7. PERFORMING ORGANIZATION NAME(S) AND ADDRESS(ES)

George C. Marshall Space Flight Center
Huntsville, AL 35812

8. PERFORMING ORGANIZATION REPORT NUMBER

M–1338

9. SPONSORING/MONITORING AGENCY NAME(S) AND ADDRESS(ES)

National Aeronautics and Space Administration
Washington, DC 20546–0001

10. SPONSORING/MONITOR'S ACRONYM(S)

NASA

11. SPONSORING/MONITORING REPORT NUMBER

NASA/TM—2012–217462

12. DISTRIBUTION/AVAILABILITY STATEMENT

Unclassified-Unlimited
Subject Category 33
Availability: NASA CASI (443–757–5802)

13. SUPPLEMENTARY NOTES

Prepared for the Space Systems Department/Engineering Directotrate

14. ABSTRACT

NASA analyzes electrical, electronic, and electromechanical (EEE) parts used in space vehicles to understand failure modes of these components. Operational amplifiers and transistors are two examples of EEE parts critical to NASA missions that can fail due to electrical overstress (EOS). EOS is the result of voltage or current over time conditions that exceeds a component's specification limit. The objective of this study was to provide known voltage pulses over well-defined time intervals to determine the type and extent of damage imparted to the device. The amount of current was not controlled but measured so that pulse energy was determined. The damage was ascertained electrically using curve trace plots and optically using various metallographic techniques. The resulting data can be used to build a database of physical evidence to compare to damaged components removed from flight avionics. The comparison will provide the avionics failure analyst necessary information about voltage and times that caused flight or test failures when no other electrical data is available.

15. SUBJECT TERMS

electrical overstress; failure analysis; electrical, electronic, electromechanical parts; curve tracer; pulse generator

16. SECURITY CLASSIFICATION OF:			17. LIMITATION OF ABSTRACT	18. NUMBER OF PAGES	19a. NAME OF RESPONSIBLE PERSON
a. REPORT	b. ABSTRACT	c. THIS PAGE			STI Help Desk at email: help@sti.nasa.gov
U	U	U	UU	48	19b. TELEPHONE NUMBER *(Include area code)* STI Help Desk at: 443–757–5802

National Aeronautics and
Space Administration
IS20
George C. Marshall Space Flight Center
Huntsville, Alabama 35812